


Kinetics of Isothermal Reactive Diffusion Between Solid Cu and Liquid Sn

M. O ¹, T. SUZUKI,² and M. KAJIHARA^{1,3}

1.—Department of Materials Science and Engineering, Tokyo Institute of Technology, Yokohama 226-8502, Japan. 2.—Graduate School, Tokyo Institute of Technology, Yokohama 226-8502, Japan. 3.—e-mail: kajihara@materia.titech.ac.jp

The Cu/Sn system is one of the most fundamental and important metallic systems for solder joints in electric devices. To realize reliable solder joints, information on reactive diffusion at the solder joint is very important. In the present study, we experimentally investigated the kinetics of the reactive diffusion between solid Cu and liquid Sn using semi-infinite Cu/Sn diffusion couples prepared by an isothermal bonding technique. Isothermal annealing of the diffusion couple was conducted in the temperature range of 533–603 K for various times up to 172.8 ks (48 h). Using annealing, an intermetallic layer composed of Cu_6Sn_5 with scallop morphology and Cu_3Sn with rather uniform thickness is formed at the original Cu/Sn interface in the diffusion couple. The growth of the Cu_6Sn_5 scallop occurs much more quickly than that of the Cu_3Sn layer and thus predominates in the overall growth of the intermetallic layer. This tendency becomes more remarkable at lower annealing temperatures. The total thickness of the intermetallic layer is proportional to a power function of the annealing time, and the exponent of the power function is close to unity at all the annealing temperatures. This means that volume diffusion controls the intermetallic growth and the morphology of the Cu_6Sn_5 /Sn interface influences the rate-controlling process. Adopting a mean value of 0.99 for the exponent, we obtain a value of 26 kJ/mol for the activation enthalpy of the intermetallic growth.

Key words: Reactive diffusion, intermetallic compounds, soldering, bulk diffusion, Cu-Sn system

INTRODUCTION

Copper is widely used as a conducting material for the metallization layer in electronics devices due to its high electrical and thermal conductivities. On the other hand, various Sn-base alloys are preferentially utilized as Pb-free solders owing to their low melting temperatures. At the joint between the Cu metallization and the Sn-base solder, an intermetallic layer consisting of Cu_6Sn_5 and Cu_3Sn is formed during soldering, and then gradually grows during energization heating at solid-state temperatures.^{1–11} Since such an intermetallic layer is brittle

and possesses high electrical resistivity, the intermetallic growth gradually degrades the mechanical and electrical properties of the joint.

The reactive diffusion between solid Cu and liquid Sn was observed at a temperature of $T = 553$ K by Bartels et al.¹² using Cu/Sn/Cu diffusion couples prepared by an isothermal solidification technique. This technique was also used by Li et al.¹³ to observe the reactive diffusion at temperatures of 533 K, 573 K, and 613 K. Both observations indicate that an intermetallic layer composed of Cu_6Sn_5 and Cu_3Sn is produced at the original Cu/Sn interface in the diffusion couple in the early stages, and that Sn and Cu_6Sn_5 are finally depleted in the later stages.^{12,13} In contrast, an immersion technique was used by Takaku et al.¹⁴ to observe the

reactive diffusion at temperatures of 523 K, and 573 K. During annealing, an intermetallic layer consisting of Cu_6Sn_5 and Cu_3Sn is formed at the original Cu/Sn interface in the diffusion couple, where the thickness of the Cu_3Sn layer is smaller than that of the Cu_6Sn_5 layer. According to their result,¹⁴ the total thickness of the intermetallic layer is proportional to the square root of the annealing time. This relationship is usually called a parabolic relationship.¹⁵ However, the proportionality coefficient of a parabolic relationship is greater at longer annealing times than at shorter annealing times. This means that the growth of the intermetallic layer is accelerated at longer annealing times. The growth of the compound layer can be controlled by the interdiffusion and the interface reaction at the moving interface. Here, the parabolic relationship indicates volume diffusion or boundary diffusion without grain growth in the interdiffusion coefficient. Nevertheless, any acceleration mechanisms for the parabolic relationship are not yet known.

The kinetics of the growth behavior due to the reactive diffusion between various solid and liquid metals has been observed experimentally using an isothermal bonding (IB) technique in previous studies.^{16–21} In this technique, the solid and liquid metals are separately preheated in a vacuum. After sufficiently long preheating, both metals are brought into contact with each other, and then isothermally annealed at the same temperature as the preheating. Therefore, unlike an immersion technique, the temperatures of the solid and liquid metals become equivalent during preheating and remain constant during reactive diffusion after bonding.²¹ In the present study, the IB technique was used to investigate the kinetics of the reactive diffusion between solid Cu and liquid Sn. Semi-infinite Cu/Sn diffusion couples were prepared by the IB technique, and then isothermally annealed in the temperature range of 533–603 K. The microstructure of the annealed diffusion couple was observed in a metallographical manner. The rate-controlling process of the reactive diffusion is discussed on the basis of the observations.²¹

EXPERIMENTAL

A commercial polycrystalline rod of pure Cu with a diameter of 8 mm and purity higher than 99.9% was purchased from Nilaco and cut into columnar specimens with lengths of 5 mm in a manner similar to previous studies.^{18,21} Each columnar specimen was annealed at a temperature of 1173 K for a time of 2 h in a vacuum, followed by slow cooling. The top and bottom flat surfaces of the annealed columnar specimen were mechanically polished on # 800–4000 emery papers.

Columnar specimens with length of 30 mm were cut from a rod of pure Sn with a diameter of 6 mm and purity of 99.9% purchased from Nilaco.^{18,20,21} A

columnar Sn specimen and a mechanically polished Cu specimen were encapsulated in an evacuated silica capsule with an inner diameter of 8.5 mm. The silica capsule was isothermally preheated for 1.8 ks (0.5 h) in the temperature range of 533–603 K using a commercial muffle furnace, where the solid Cu was separated from the molten Sn. After sufficient preheating, a flat surface of the solid Cu was immediately brought into contact with that of the molten Sn with a diameter of 8.5 mm and length of 15 mm to prepare a columnar solid-Cu/liquid-Sn diffusion couple. The diffusion couple was isothermally annealed for various times up to 172.8 ks (48 h) at the same temperature as the preheating, followed by water quenching with breaking the capsule. The annealing temperature and time are denoted by T and t , respectively.²¹

Emery papers of # 800–4000 and alumina with diameters of 1 μm , 0.3 μm and 0.05 μm were used to mechanically polish cross-sections of the annealed diffusion couples. The mechanically polished cross-sections were finished with colloidal silica suspension (OPS liquid manufactured by Struers). The microstructure of the cross-sections was observed by differential interference contrast optical microscopy (DICOM) and with secondary electron image (SEI) by field emission scanning electron microscopy (FESEM). The DICOM and FESEM observations were carried out using OPTIPHOT (Nikon) and JSM-7000F (JEOL), respectively. Concentrations of Cu and Sn in each phase on the cross-section were measured by electron probe microanalysis (EPMA) using pure Cu and Sn with a purity of 99.99% as standard specimens. The EPMA measurement was conducted utilizing JXA8900RL (JEOL) under the following conditions: the accelerating voltage was 20 kV; the probe current was 5 nA; the analyzing crystals for Cu-K α and Sn-L α were lithium fluoride (LiF) and polyethylene terephthalate (PET), respectively; and the chemical composition was evaluated by a standard ZAF correction technique.²¹

RESULTS AND DISCUSSION

Microstructure

Figure 1a shows an SEI micrograph of a diffusion couple annealed at $T = 563$ K for $t = 172.8$ ks (48 h), and Fig. 1b indicates that of a diffusion couple annealed at $T = 603$ K for $t = 172.8$ ks (48 h). In Fig. 1, the lower region is the Cu specimen, and the upper region is the Sn specimen. As can be seen, two phases with different contrasts and shapes are recognized between the Cu and the Sn. Concentration profiles of Cu and Sn across the two phases along the direction normal to the original Cu/Sn interface were measured to identify each phase by EPMA. Figure 2 represents a result of the EPMA measurement for a diffusion couple with $T = 583$ K, and $t = 172.8$ ks (48 h). In this figure, the vertical and horizontal axes show the mol fraction y_i of component i and the distance x ,

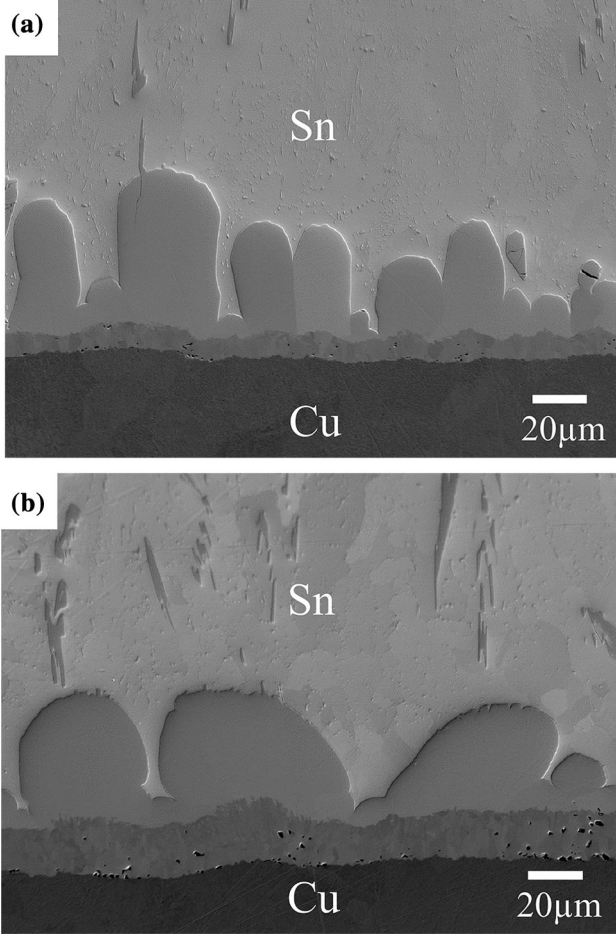


Fig. 1. Cross-sectional SEI micrographs of the Cu/Sn diffusion couples annealed for $t = 172.8$ ks (48 h): (a) $T = 563$ K, and (b) $T = 603$ K.

respectively, and open squares and circles indicate the mol fractions y_{Cu} and y_{Sn} , respectively. Here, the origin $x = 0$ of the distance is located in the Sn. The location of the origin is discretionally chosen to conveniently represent the concentration profiles, because attention is focused on phase identification for the EPMA measurement. As can be seen in Fig. 2, the phase with scallop morphology on the Sn side is $\eta\text{-Cu}_6\text{Sn}_5$, and that with rather uniform thickness on the Cu side is $\varepsilon\text{-Cu}_3\text{Sn}$. In contrast, small voids are distributed in the Cu_3Sn layer but not in the Cu_6Sn_5 scallop. We may consider that the voids in the Cu_3Sn layer are formed by the Kirkendall effect. In a previous study,²² the void formation in the Cu_3Sn layer due to the Kirkendall effect was quantitatively analyzed using an analytical diffusion model. According to phase diagrams in the binary Cu-Sn system,^{23–25} $\eta\text{-Cu}_6\text{Sn}_5$ and $\varepsilon\text{-Cu}_3\text{Sn}$ are stable compounds at $T = 533\text{--}603$ K. Thus, all the stable compounds at the annealing temperatures are produced in the diffusion couple. Such a microstructure was observed in all the annealed diffusion couples.

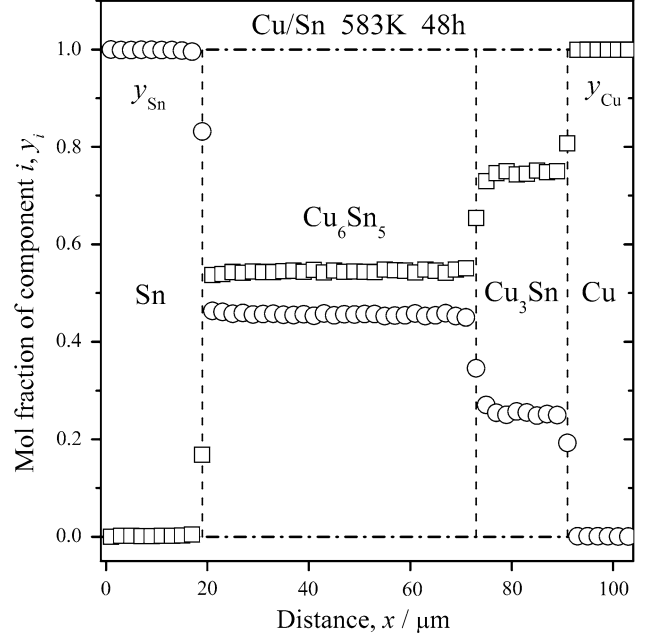


Fig. 2. Concentration profiles of Cu and Sn across the intermetallic layer for the Cu/Sn diffusion couple annealed at $T = 583$ K for $t = 172.8$ ks (48 h).

Growth Behavior of Intermetallic Layer

In cross-sectional DICOM images, like the SEI micrographs in Fig. 1, an intermetallic layer composed of Cu_6Sn_5 and Cu_3Sn is distinguishable from the Cu and Sn. Figure 3 shows the schematic microstructure of the intermetallic layer at cross-section i . The area A_i of the intermetallic layer corresponding to the partial length w_i of the original Cu/Sn interface in Fig. 3 was measured for each cross-sectional DICOM image, and then the sums A and w were obtained as^{20,21}

$$A = \sum_{i=1}^m A_i \quad (1a)$$

and

$$w = \sum_{i=1}^m w_i \quad (1b)$$

from A_i and w_i , respectively, where $m \geq 5$. Using the values of A and w , the total thickness l of the intermetallic layer was evaluated at each annealing time t by the following equation:^{20,21}

$$l = \frac{A}{w}. \quad (2)$$

The results for $T = 533$ K, 563 K, 583 K, and 603 K are indicated in Fig. 4 as open triangles, rhombuses, squares and circles, respectively. In this figure, the vertical and horizontal axes show the thickness l and the annealing time t , respectively. Here, both axes are indicated in logarithmic scales. As can be seen, the experimental points are located on a

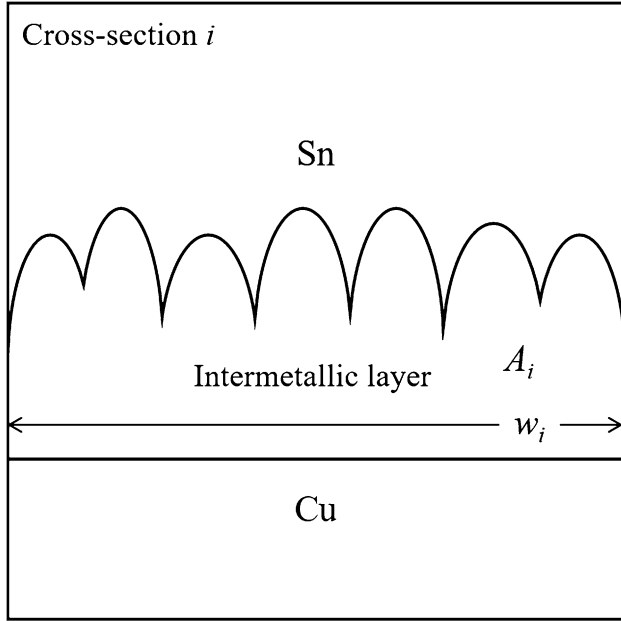


Fig. 3. Schematic of morphology for the intermetallic layer on cross-section i .

straight line at each annealing temperature. This means that l is expressed as a power function of t by the following equation.²⁶

$$l = k \left(\frac{t}{t_0} \right)^n \quad (3)$$

Here, t_0 is unit time, 1 s, which is adopted to make the argument t/t_0 of the power function dimensionless. The proportionality coefficient k has the same dimension as the thickness l , but the exponent n is dimensionless.²⁶ As pointed out in previous studies,^{20,21,27,28} the dimensionless argument of the power function is essentially important, otherwise the dimension of k varies depending on the value of n . From the experimental points in Fig. 4, k and n were evaluated by the least-squares method as shown with various straight lines.^{27,28} The overall growth rate of the intermetallic layer monotonically increases with increasing annealing temperature T at $T = 533\text{--}603$ K.

The interface between the Cu_6Sn_5 scallop and the Cu_3Sn layer is well distinguishable in the DICOM and SEI micrographs. The mean thickness l_i of each compound was evaluated using the relationships similar to Eqs. 1a, 1b, and 2. Thus, there exists the following relationship between l_1 , l_2 and l .²⁸

$$l = l_1 + l_2 \quad (4)$$

Here, l_1 is the mean thickness of the Cu_6Sn_5 scallop, and l_2 is that of the Cu_3Sn layer. The values of l , l_1 and l_2 are plotted in Fig. 5 against the annealing time t as open circles, squares and rhombuses, respectively. Figure 5a, b, c, and d indicates the results for $T = 533$ K, 563 K, 583 K, and 603 K, respectively. In Fig. 5, like Fig. 4, the vertical and

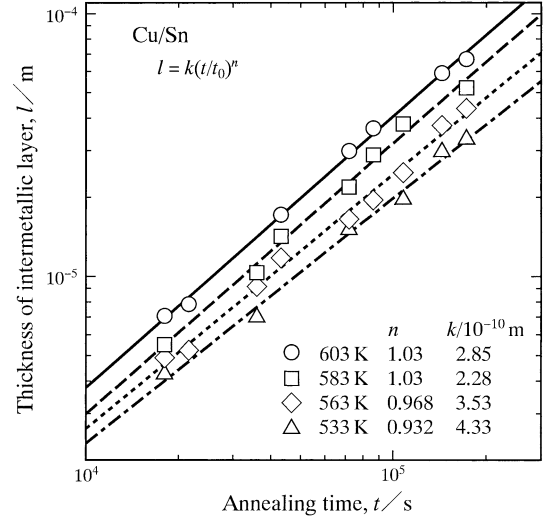


Fig. 4. The total thickness l of the intermetallic layer versus the annealing time t at $T = 533$ K, 563 K, 583 K, and 603 K shown as open triangles, rhombuses, squares and circles, respectively.

horizontal axes indicate the logarithms of l_i and t , respectively, and the open symbols lie well on a straight line for each compound. Therefore, l_i is expressed as a power function of t by the following equation of the same formula as Eq. 3.²⁷

$$l_i = k_i \left(\frac{t}{t_0} \right)^n \quad (5)$$

From the experimental points in Fig. 5, k_i and n for l_i in Eq. 5 were evaluated by the least-squares method as shown with various straight lines. According to the evaluation at $T = 533\text{--}603$ K, the growth rate of the Cu_3Sn layer is much smaller than that of the Cu_6Sn_5 scallop. However, the exponent n is slightly greater for the Cu_3Sn layer than for the Cu_6Sn_5 scallop. This implies that the difference in the growth rate between the Cu_6Sn_5 scallop and the Cu_3Sn layer lightly decreases with increasing annealing time. To estimate the annealing time dependence of the growth rate difference, the ratio r_i of the thickness l_i to the total thickness l was evaluated by the following equation.

$$r_i = \frac{l_i}{l} \quad (6)$$

The results for $T = 533$ K, 563 K, 583 K, and 603 K are shown in Fig. 6a, b, c, and d, respectively. In Fig. 6, the vertical and horizontal axes indicate the ratio r_i and the annealing time t , respectively, and open circles and squares represent the ratio r_1 of the Cu_6Sn_5 scallop and r_2 of the Cu_3Sn layer, respectively. As can be seen, r_1 is greater than r_2 within the experimental annealing times at $T = 533\text{--}603$ K. Although the open symbols are slightly scattered, the difference between r_1 and r_2 gradually decreases with increasing annealing time t at most of the annealing temperatures. The mean

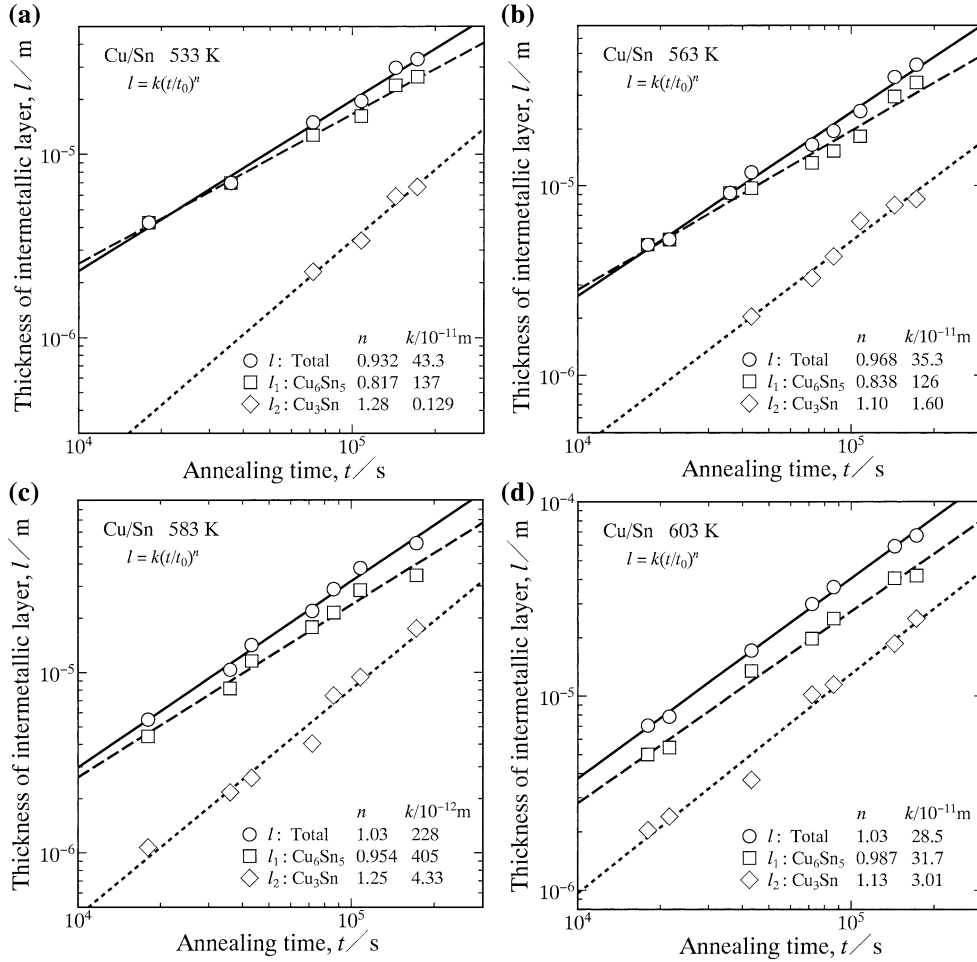


Fig. 5. The thicknesses l , l_1 and l_2 versus the annealing time t shown as open circles, squares and rhombuses, respectively: (a) $T = 533$ K, (b) $T = 563$ K, (c) $T = 583$ K, and (d) $T = 603$ K.

values of r_1 and r_2 are plotted against the annealing temperature T as open circles and squares, respectively, with error bars in Fig. 7. Here, the error bar represents the standard error.²⁷ As the annealing temperature T increases, the mean value of r_2 increases, but that of r_1 decreases. This means that the difference in the growth rate between the Cu_6Sn_5 scallop and the Cu_3Sn layer monotonically decreases with increasing annealing temperature.²⁷

As briefly mentioned in the “Introduction”, the reactive diffusion between solid Cu and liquid Sn was experimentally observed by Takaku et al.¹⁴ In their experiment, Cu/Sn diffusion couples were prepared by an immersion technique and then annealed at temperatures of $T = 523$ K, and 573 K. According to their observation, an intermetallic layer consisting of Cu_6Sn_5 and Cu_3Sn is formed at the original Cu/Sn interface in the diffusion couple during annealing. The thicknesses l , l_1 and l_2 for $T = 523$ K reported by Takaku et al.¹⁴ are plotted in Fig. 8 against the annealing time t as open circles, squares and rhombuses, respectively. Also in Fig. 8, the power relationship holds between the thicknesses l , l_1 and l_2 and the annealing time t ,

although the open symbols are slightly scattered. Furthermore, l_2 is smaller than l_1 within the experimental annealing times. In their article,¹⁴ the parabolic relationship was used to estimate the dependencies of l , l_1 and l_2 on t . In such dependencies, the parabolic relationship holds, but the parabolic coefficient is greater at longer annealing times than at shorter annealing times. This shows that the intermetallic growth is accelerated at longer annealing times. Nevertheless, any acceleration mechanisms for the parabolic relationship are not so far known. On the other hand, in Fig. 8, the dependencies of l , l_1 and l_2 on t are reasonably expressed by the power relationship. As can be seen, n is close to unity for l_2 , but takes intermediate values between 0.5 and unity for l and l_1 . The mean values of r_1 and r_2 estimated from the open symbols in Fig. 8 are plotted in Fig. 7 against the annealing temperature T as an open rhombus and triangle, respectively, with error bars. The difference in the exponent n between the thicknesses l_1 and l_2 is much greater for the result in Fig. 8 than for that in Fig. 5. Hence, the standard error is greater for the open rhombus and triangle than for the open circles

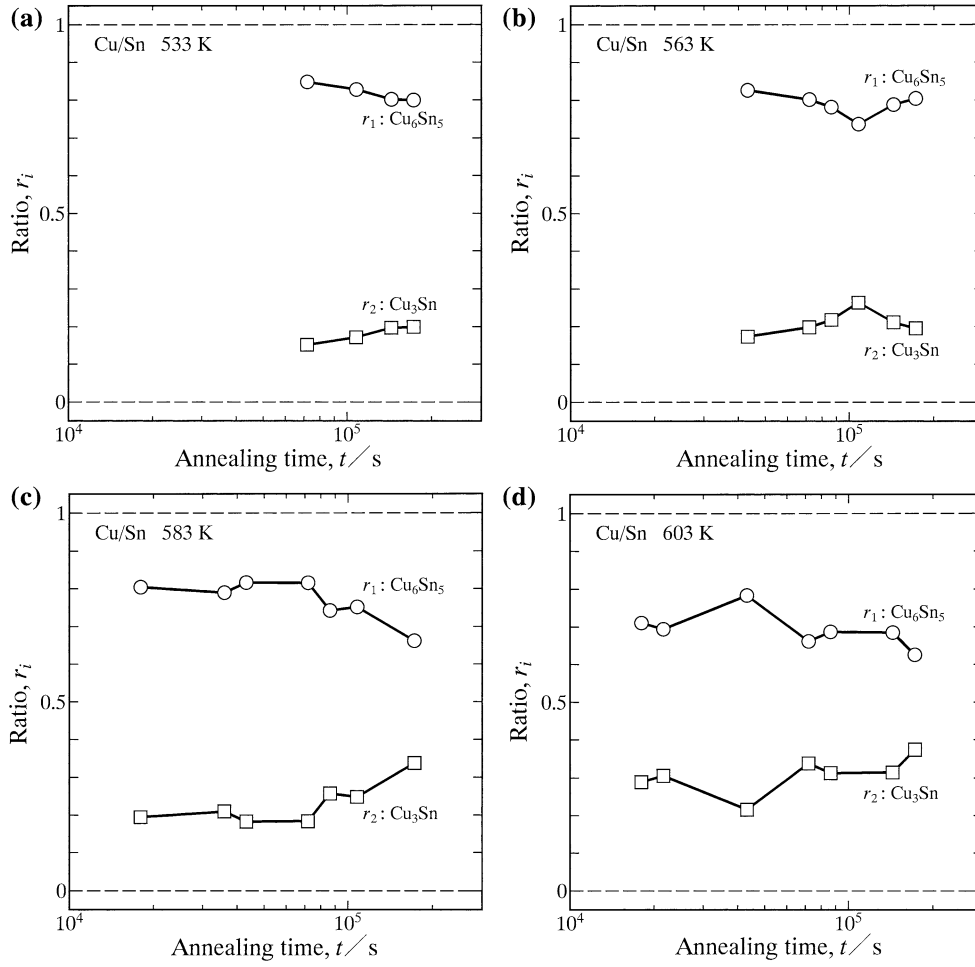


Fig. 6. The ratio r_i versus the annealing time t shown as open circles and squares for Cu_6Sn_5 and Cu_3Sn , respectively: (a) $T = 533$ K, (b) $T = 563$ K, (c) $T = 583$ K, and (d) $T = 603$ K.

and squares in Fig. 7. However, the open rhombus and triangle do not necessarily contradict the temperature dependencies of r_1 and r_2 for the open circles and squares, respectively.

The reactive diffusion between solid Cu and liquid Sn was also experimentally observed by Li et al.¹³ In that experiment, sandwich Cu/Sn/Cu diffusion couples were prepared by an isothermal solidification technique and then annealed for various times at temperatures of $T = 533$ K, 573 K, and 613 K. Here, the initial thickness is $25 \mu\text{m}$ and $100 \mu\text{m}$ for the Sn and Cu foils, respectively, in the Cu/Sn/Cu diffusion couple. Their observation shows that an intermetallic layer composed of Cu_6Sn_5 and Cu_3Sn is formed at the original Cu/Sn interface in the diffusion couple in the early stages, and Cu_6Sn_5 and the Sn foil are finally depleted in the later stages. The values of l for $T = 533$ K, 573 K, and 613 K reported by Li et al.¹³ are plotted in Fig. 9 against the annealing time t as open rhombuses, squares and circles, respectively. As can be seen, the open symbols are much more scattered in Fig. 9 than in Fig. 4. This may be attributed to smaller values of l corresponding to shorter annealing times in Fig. 9

than in Fig. 4. For the Cu/Sn diffusion couple in the present study, the initial thickness d_{Sn} of the Sn and that d_{Cu} of the Cu are 15 mm and 5 mm , respectively. For such values of d_{Sn} and d_{Cu} , the Cu/Sn diffusion couple is practically considered to be a semi-infinite diffusion couple within the experimental annealing times at $T = 533$ – 603 K.^{20,21} In contrast, each half of the sandwich Cu/Sn/Cu diffusion couple prepared by Li et al.¹³ corresponds to the Cu/Sn diffusion couple with $d_{\text{Sn}} = 12.5 \mu\text{m}$ and $d_{\text{Cu}} = 100 \mu\text{m}$. Since d_{Sn} is three orders of magnitude smaller for the Cu/Sn/Cu diffusion couple than for the semi-infinite Cu/Sn diffusion couple, soft impingement of interdiffusion field occurs in the Sn foil of the Cu/Sn/Cu diffusion couple even in the early stages. Therefore, the boundary conditions are dissimilar between the Cu/Sn/Cu diffusion couple and the semi-infinite Cu/Sn diffusion couple. Assuming that the power relationship between l and t also holds in Fig. 9, we obtain values of $n = 0.22$, 0.41 and 0.30 for $T = 533$ K, 573 K, and 613 K, respectively. As mentioned earlier, for the Cu/Sn/Cu diffusion couple, the intermetallic layer is formed in the early stages, and then Cu_6Sn_5 and the

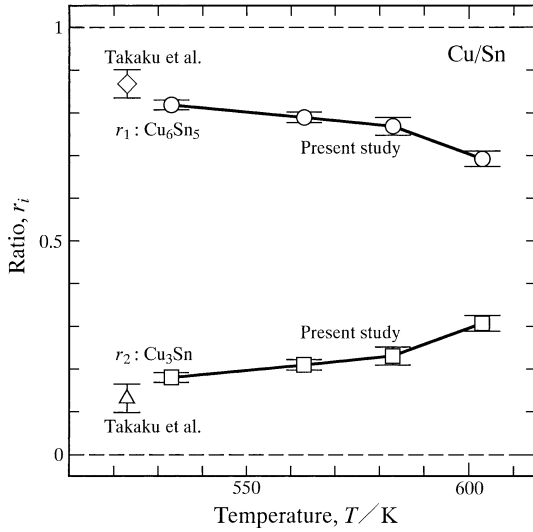


Fig. 7. The mean value of the ratio r_i versus the annealing temperature T shown as open circles and squares with error bars for Cu_6Sn_5 and Cu_3Sn , respectively. The corresponding results obtained from the observation reported by Takaku et al.¹⁴ are also indicated as open rhombus and triangle with error bars for Cu_6Sn_5 and Cu_3Sn , respectively.

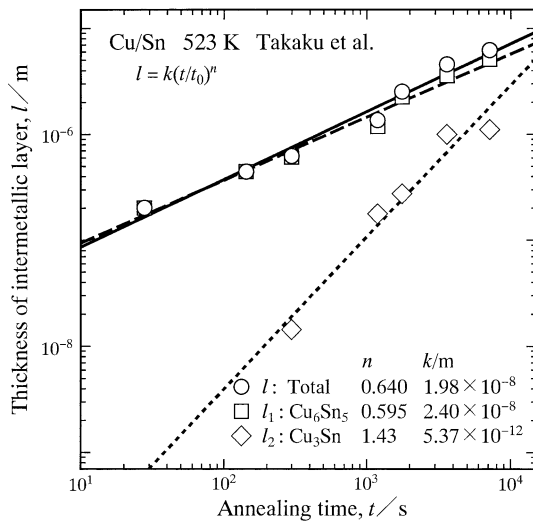


Fig. 8. The thicknesses l , l_1 and l_2 versus the annealing time t at $T = 523$ K shown as open circles, squares and rhombuses, respectively, for the observations reported by Takaku et al.¹⁴

Sn foil are finally depleted in the later stages. Therefore, growth mechanisms of Cu_6Sn_5 and Cu_3Sn vary depending on the annealing time. The values of n smaller than 0.5 may be attributed to such annealing time dependencies of the growth mechanisms.

Rate-Controlling Process

The values of the exponent n in Fig. 4 are plotted in Fig. 10 against the annealing temperature T as open circles with error bars. As can be seen, n is rather insensitive to T and close to unity at

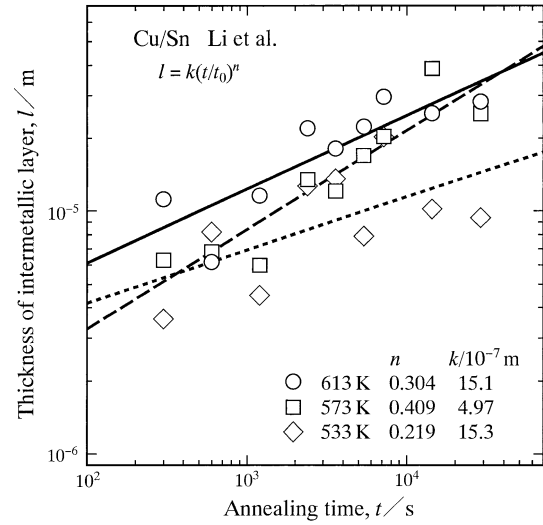


Fig. 9. The total thickness l of the intermetallic layer versus the annealing time t shown as open rhombuses, squares and circles for $T = 533$ K, 573 K, and 613 K, respectively, for the observations reported by Li et al.¹³

$T = 533$ – 603 K. When the layer growth is governed by volume diffusion, n is equal to 0.5.^{29–37} This is called the parabolic relationship as mentioned earlier. For precipitation of a second phase into an untransformed matrix in binary alloy systems, the growth of the second phase controlled by volume diffusion usually obeys the parabolic relationship.²¹ If the shape of the second phase is a paraboloid of revolution or a parabolic cylinder, however, the longitudinal growth of the second phase occurs according to the linear relationship even for the volume diffusion rate-controlling process.^{38–42} Here, the linear relationship means that the length of the second phase increases in proportion to the annealing time. As shown in Fig. 7, the ratio r_1 of the Cu_6Sn_5 scallop is much greater than that r_2 of the Cu_3Sn layer. Thus, the growth of the Cu_6Sn_5 scallop into the Sn liquid mainly controls the overall growth behavior of the intermetallic layer. As a result, the overall growth rate of the intermetallic layer is mainly determined by the migration of the $\text{Cu}_6\text{Sn}_5/\text{Sn}$ interface. According to the SEI micrographs in Fig. 1, the $\text{Cu}_6\text{Sn}_5/\text{Sn}$ interface is considerably gathered. The values of n close to unity in Fig. 10 may be attributed to such gathered morphology of the $\text{Cu}_6\text{Sn}_5/\text{Sn}$ interface. The relationship between the moving-interface morphology and the exponent n in Eq. 3 has been discussed in previous studies.^{20,21} As previously mentioned, the power relationship between l and t also holds for the result by Takaku et al.¹⁴ According to the result in Fig. 8, $n = 0.64$ for l . Such an intermediate value of n between 0.5 and unity implies that volume diffusion mainly controls the intermetallic growth and the gathered morphology of the $\text{Cu}_6\text{Sn}_5/\text{Sn}$ interface partially influences the exponent of the power function.

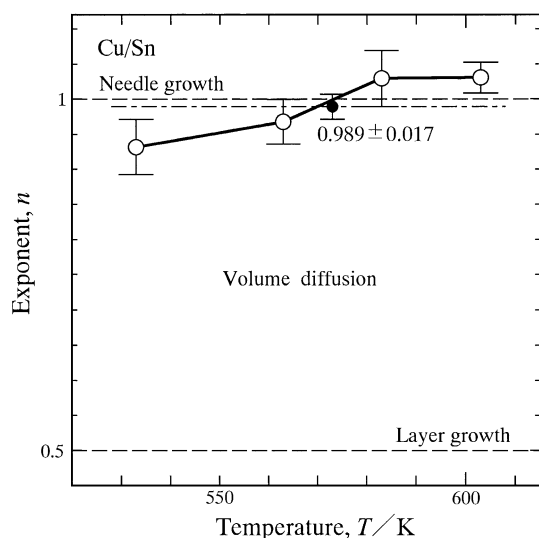


Fig. 10. The exponent n versus the annealing temperature T .

As shown by the open circles in Fig. 10, n is somewhat independent of T . Considering a common value of n at all the annealing temperatures, k and n were evaluated from the experimental points in Fig. 4 by the least-squares method. The evaluated value of n is shown in Fig. 10 as a solid circle with error bars, and those of k are plotted in Fig. 11 against T as open circles with error bars. In Fig. 11, the vertical axis indicates the logarithm of k , and the horizontal axis shows the reciprocal of T . As can be seen in Fig. 11, the open circles are well located on a straight line within experimental uncertainty, and hence the dependence of k on T is expressed by the following equation.²¹

$$k = k_0 \exp\left(-\frac{Q_k}{RT}\right) \quad (7)$$

Here, k_0 is the pre-exponential factor, Q_k is the activation enthalpy, and R is the gas constant. The values of k_0 and Q_k were evaluated from the open circles by the least-squares method as shown by a solid line in Fig. 11. The evaluation provides $Q_k = 26$ kJ/mol. This value of Q_k corresponds to the activation enthalpy for the intermetallic growth with parabolic-cylinder morphology controlled by volume diffusion.

CONCLUSIONS

To investigate the kinetics of the reactive diffusion in the solid-Cu/liquid-Sn system, Cu/Sn diffusion couples were prepared by the isothermal bonding technique and then annealed for various periods at temperatures of $T = 533$ – 603 K. In this temperature range, Cu_6Sn_5 and Cu_3Sn are the stable compounds in the binary Cu-Sn system.^{23–25} During annealing, the intermetallic layer consisting of the Cu_6Sn_5 scallop and the Cu_3Sn layer is produced at the original Cu/Sn interface in the

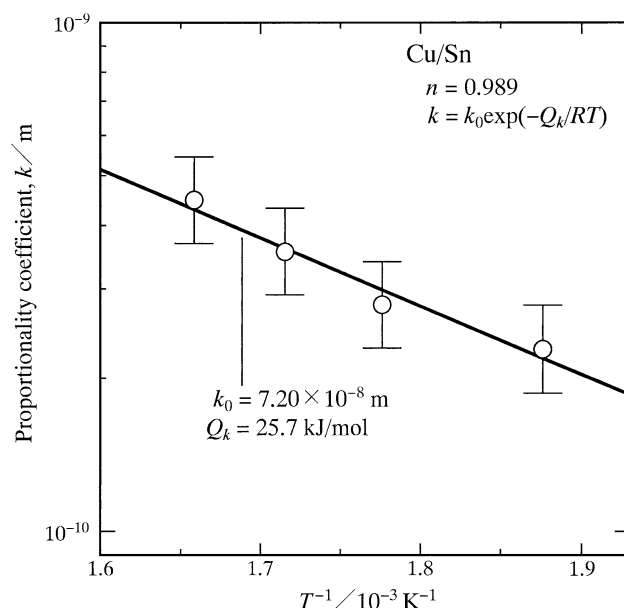


Fig. 11. The proportionality coefficient k versus the annealing temperature T .

diffusion couple. Here, the mean thickness of the Cu_6Sn_5 scallop is greater than that of the Cu_3Sn layer. Hence, the Cu_6Sn_5 scallop predominates in the overall intermetallic growth. The total thickness of the intermetallic layer increases in proportion to a power function of the annealing time. If the growth of a compound with a parabolic-cylinder shape is controlled by volume diffusion, the exponent n of the power function is equal to unity. According to the observations, n is close to unity at all the annealing temperatures. Thus, the intermetallic growth is controlled by volume diffusion.

ACKNOWLEDGEMENTS

The authors are grateful to Dr. Y. Tanaka at Tokyo Institute of Technology, Japan, for stimulating discussions. The present study was partially supported by a Grant-in-Aid for Scientific Research from the Ministry of Education, Culture, Sports, Science and Technology of Japan.

REFERENCES

1. L. Zakraysek, *Weld. Res. Suppl.* 51, 536 (1972).
2. K.N. Tu, *Acta Metall. Mater.* 21, 347 (1973).
3. M. Onishi and H. Fujibuchi, *Trans. JIM* 16, 539 (1975).
4. H.N. Keller, *IEEE Trans. Compon. Hybrids Manuf. Technol.* 2, 180 (1979).
5. H.N. Keller and J.M. Morabito, *Surf. Interface Anal.* 3, 16 (1981).
6. J.O.G. Parent, D.D.L. Chung, and I.M. Bernstein, *J. Mater. Sci.* 23, 2564 (1988).
7. A.J. Sunwoo, J.W. Morris, and G.K. Lucey, *Metall. Trans. A* 23, 1323 (1992).
8. P.T. Vianco, P.F. Hlava, and A.C. Kilgo, *J. Electron. Mater.* 23, 583 (1994).
9. D.R. Frear and P.T. Vianco, *Metall. Mater. Trans. A* 25, 1509 (1994).
10. S. Choi, T.R. Bieler, J.P. Lucas, and K.N. Subramanian, *J. Electron. Mater.* 28, 1209 (1999).

11. T. Takenaka, S. Kano, M. Kajihara, N. Kurokawa, and K. Sakamoto, *Mater. Sci. Eng. A Struct.* 396, 115 (2005).
12. F. Bartels, J.W. Morris, G. Dalke, and W. Gust, *J. Electron. Mater.* 23, 787 (1994).
13. J.F. Li, P.A. Agyakwa, and C.M. Johnson, *Acta Mater.* 59, 1198 (2011).
14. Y. Takaku, X.J. Liu, I. Ohnuma, R. Kainuma, and K. Ishida, *Mater. Trans.* 45, 646 (2004).
15. M. Mita, M. Kajihara, N. Kurokawa, and K. Sakamoto, *Mater. Sci. Eng. A Struct.* 403, 269 (2005).
16. Y. Tanaka and M. Kajihara, *Mater. Sci. Eng. A Struct.* 459, 101 (2007).
17. Y. Tanaka and M. Kajihara, *J. Mater. Sci.* 45, 5676 (2010).
18. Y. Tanaka, M. Kajihara, and Y. Watanabe, *Mater. Sci. Eng. A Struct.* 445, 355 (2007).
19. Y. Tanaka and M. Kajihara, *Mater. Trans.* 50, 2212 (2009).
20. M. Hida and M. Kajihara, *Mater. Trans.* 53, 1240 (2012).
21. A. Nakane, T. Suzuki, M. O, and M. Kajihara, *Mater. Trans.* 57, 838 (2016).
22. M. O, G. Vakanas, N. Moelans, M. Kajihara, and W. Zhang, *Microelectron. Eng.* 120, 133 (2014).
23. T.B. Massalski, H. Okamoto, P.R. Subramanian, and L. Kacprzak, *Binary Alloy Phase Diagrams*, vol. 2 (Materials Park, OH: ASM International, 1990), p. 1482.
24. S. Fürtauer, D. Li, D. Cupid, and H. Flandorfer, *Intermetallics* 34, 142 (2013).
25. D. Li, P. Franke, S. Fürtauer, D. Cupid, and H. Flandorfer, *Intermetallics* 34, 148 (2013).
26. Y. Yato and M. Kajihara, *Mater. Sci. Eng. A Struct.* 428, 276 (2006).
27. Y. Takamatsu, M. O, and M. Kajihara, *Mater. Trans.* 58, 16 (2017).
28. Y. Takamatsu, M. O, and M. Kajihara, *Mater. Trans.* 58, 567 (2017).
29. M. Kajihara, *Acta Mater.* 52, 1193 (2004).
30. M. Kajihara, *Mater. Sci. Eng. A Struct.* 403, 234 (2005).
31. M. Kajihara, *Mater. Trans.* 46, 2142 (2005).
32. M. Kajihara, *Mater. Trans.* 47, 1480 (2006).
33. Y. Tanaka and M. Kajihara, *Mater. Trans.* 47, 2480 (2006).
34. M. Kajihara and T. Yamashina, *J. Mater. Sci.* 42, 2432 (2007).
35. M. Kajihara, *Mater. Trans.* 49, 715 (2008).
36. M. Kajihara, *Mater. Trans.* 51, 1242 (2010).
37. M. Kajihara, *Mater. Trans.* 53, 1896 (2012).
38. A. Papapetrou, *Z. Kristallogr.* 92, 89 (1935).
39. G.P. Ivantsov, *Dokl. Akad. Nauk SSSR.* 58, 567 (1947).
40. G. Horvay and J.W. Cahn, *Acta Metall. Mater.* 9, 695 (1961).
41. R. Trivedi, *Acta Metall. Mater.* 18, 287 (1970).
42. P.E.J. Rivera-Diaz-del-Castillo and H.K.D.H. Bhadeshia, *Mater. Sci. Technol. SER* 17, 30 (2001).